

HD-TVP-98-3

Target Fragmentation in pp and γp Collisions at High Energies

U. D'Alesio¹ and H.J. Pirner

*Institut für Theoretische Physik, Universität Heidelberg
D-69120 Heidelberg*

A. Schäfer

*Institut für Theoretische Physik, Universität Regensburg
D-93040 Regensburg*

Abstract

We calculate target fragmentation in $pp \rightarrow nX$ and $\gamma p \rightarrow nX$ reactions in the meson cloud picture of the nucleon. The $pp \rightarrow nX$ reaction is used to fix the $pn\pi^+$ form factor for three different models. We take into account the possible destruction of the residual neutron by the projectile. Using the form factor from the hadronic reaction we calculate photoproduction and small x_{Bj} electroproduction of forward neutrons at HERA. Here the $q\bar{q}$ dipoles in the photon can rescatter on the residual neutron. In photoproduction we observe about the same amount of absorption as in the hadronic reaction. For deep inelastic events ($Q^2 > 10$ GeV 2) screening is negligible. The signature for this form of color transparency is a shift of the $d\sigma/dE_n$ distribution to higher neutron energies for photofragmentation.

¹Supported by TMR programme, EU-Project FMRX-CT96-0008.

1 Introduction

In the last two decades the study of total inclusive deep inelastic scattering (DIS) processes has allowed to extract important information on the structure of hadrons. Parton distributions have been determined and scaling violations have been tested to a high level of accuracy. The QCD improved parton model has been shown to be very reliable in the presence of a hard scale.

On the other hand semi-inclusive reactions with electromagnetic probes are still less explored. They can improve our knowledge on the inner hadronic structure. Through the study of new observables characterizing these processes we may ask more detailed questions about the proton. In this case the application of perturbative QCD (pQCD) has been restricted to high p_t events, and experiments have been analyzed in terms of parton distributions and fragmentation functions.

With the HERA collider target fragmentation can be studied in a much cleaner way than with fixed target experiments. New interest has been triggered by measurements on leading neutron production performed by the ZEUS and H1 collaborations at the electron-proton collider [1, 2]. These data are currently analyzed in terms of hadronic degrees of freedom, i.e. studying the virtual pion flux in the nucleon. Thus one hopes to extract information about the pion structure function at very small x , not reachable in Drell-Yan experiments. Novel theoretical tools to include forward leading particle production in the framework of standard pQCD have been developed by Trentadue, Veneziano and Graudenz [3, 4], who introduced a new set of non-perturbative fracture functions which allow to absorb collinear singularities at leading order into the QCD coupling constant.

If we look at γ^*p reactions in the cm system, we can consider the incoming photon as a $q\bar{q}$ state that interacts with a proton made up of two color neutral components, one of which is the final state neutron. This involves quite different aspects of the nucleon than those investigated in deep inelastic inclusive scattering. Especially long range properties of the baryon can be analysed in such a process. At which length does the string connecting a quark to the residual diquark break and produce two colour neutral objects, a meson and a nucleon? This question is especially important for nuclear physics, as one wants to know what amount of the nucleon-nucleon interaction is describable in terms of meson exchange forces in the nucleus.

From the high energy point of view the determination of the pion structure function is central. The common interpretation of the $\gamma^*p \rightarrow nX$ experiment relies on the application of the meson cloud model of the nucleon together with the factorization hypothesis that allows to separate the reaction into two steps: the fragmentation process and the interaction [5, 6]. It assumes that the fragmentation process is universal, i.e. independent of the projectile which initiates fragmentation. In the following paper we will examine the validity of this factorization hypothesis carefully.

Let us consider the generic reaction with an incoming projectile a leading to neutron production i.e. $ap \rightarrow nX$ (see fig. 1). In the pion exchange model the differential cross

section is given by the product of the pion flux factor times the total $a\pi$ cross section:

$$\frac{d\sigma^{ap \rightarrow nX}}{dz dp_t^2} = F_{n\pi}(z, p_t) \sigma_{\text{tot}}^{a\pi}(s') \quad (1)$$

The flux factor $F_{n\pi}(z, p_t)$ gives the probability for the splitting of a proton into a pion-neutron system. It depends on the longitudinal momentum fraction z carried by the detected neutron and its transverse momentum² p_t . The total cross section $\sigma_{\text{tot}}^{a\pi}(s')$ is a function of s' the center of mass sub-energy squared in the $a\pi^+$ interaction.

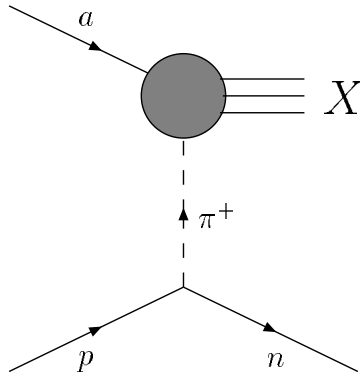


Figure 1: *Picture of semi-inclusive neutron production according to the one pion exchange model.*

The usual procedure [7, 8] is to fix the parameters entering the flux factor from the data of leading neutron production in proton-proton ($a = p$) collisions. Then assuming universality, one applies the same equation (1) to virtual photon scattering ($a = \gamma^*$) in DIS. Measuring the differential cross section $\gamma^* p \rightarrow nX$ one extracts the pion structure function, since $\sigma_{\text{tot}}^{\gamma^* \pi^+}$ is proportional to $F_2^{\pi^+}$ besides a small longitudinal contribution (see eq. (29)). Obviously the factorization hypothesis plays a crucial role in this method.

Recently a first study of absorptive corrections in the Regge formalism [9] has appeared. These absorptive effects depend on the projectile and are a source of factorization breaking. They can be comparable or even more important than other background contributions, already estimated, reducing the accuracy of $F_2^{\pi^+}$ measurements. We will investigate the relevance of absorptive corrections in detail in order to understand the one pion exchange mechanism and the extraction of the pion structure function. We apply high energy Glauber theory to calculate and compare the screening corrections in leading neutron production for pp and $\gamma^* p$ reactions. We especially search for differences between photoproduction and deep inelastic scattering in neutron fragmentation. To this end we follow the Q^2 evolution of the fracture functions from a kinematic region where the perturbative evolution of [3, 4] is not yet applicable to large Q^2 . Remarkably, we encounter a color transparency phenomenon: with increasing Q^2 the absorptive correction disappears. This effect seems to be indicated in the data [1, 10].

²We use $p_t = |\mathbf{p}_t|$.

The outline of the paper is as follows. In section 2 we describe the meson cloud model, in section 3 we calculate the absorptive corrections to $pp \rightarrow nX$. Section 4 is devoted to real and virtual photoproduction of forward neutrons. Section 5 closes with a summary and a discussion.

2 Meson Cloud Model

In this section we review briefly the main features of the meson cloud model (MCM). In the MCM a proton is viewed as a bare proton surrounded by a virtual meson cloud,

$$\begin{aligned}
|p \uparrow\rangle &= \sqrt{S} \left\{ |p_0 \uparrow\rangle + \sum_{\lambda\lambda'} \sum_{BM} \int dz d^2\mathbf{p}_t \phi_{BM}^{\lambda\lambda'}(z, \mathbf{p}_t) |B, M; z, \mathbf{p}_t\rangle \right\} \\
&= \sqrt{S} \left\{ |p_0 \uparrow\rangle + \sum_{\lambda\lambda'} \int dz d^2\mathbf{p}_t \phi_{N\pi}^{\lambda\lambda'}(z, \mathbf{p}_t) \left[\sqrt{\frac{1}{3}} |p, \pi^0; z, \mathbf{p}_t\rangle \right. \right. \\
&\quad \left. \left. + \sqrt{\frac{2}{3}} |n, \pi^+; z, \mathbf{p}_t\rangle \right] + \dots \right\}
\end{aligned} \tag{2}$$

where $\phi_{BM}^{\lambda\lambda'}(z, \mathbf{p}_t)$ is the probability amplitude to find, inside a proton with spin up, a baryon B with longitudinal momentum fraction z , transverse momentum \mathbf{p}_t and helicity λ and a meson M , with longitudinal momentum fraction $1 - z$, transverse momentum $-\mathbf{p}_t$ and helicity λ' . We restrict ourselves to the first contributions of this expansion in terms of Fock states. \sqrt{S} is the renormalization constant, which is fixed by $\langle p|p\rangle = 1$ and gives the amplitude for the bare proton.

In the light-cone approach the amplitudes $\phi_{N\pi}$, for a proton with spin $+1/2$, read [11]

$$\begin{aligned}
\phi_{N\pi}^{1/2,0}(z, \mathbf{p}_t) &= \frac{\sqrt{3}g_0}{4\pi\sqrt{\pi}} \frac{1}{\sqrt{z^2(1-z)}} \frac{m_N(z-1)}{M_{N\pi}^2 - m_N^2} \\
\phi_{N\pi}^{-1/2,0}(z, \mathbf{p}_t) &= \frac{\sqrt{3}g_0}{4\pi\sqrt{\pi}} \frac{1}{\sqrt{z^2(1-z)}} \frac{|\mathbf{p}_t| e^{-i\varphi}}{M_{N\pi}^2 - m_N^2},
\end{aligned} \tag{3}$$

where $M_{N\pi}^2$ is the invariant mass of the pion-nucleon system, given by

$$M_{N\pi}^2 = \frac{m_N^2 + p_t^2}{z} + \frac{m_\pi^2 + p_t^2}{1-z},$$

m_N and m_π are the nucleon and the pion masses; g_0 is the bare pion-nucleon coupling constant and φ is the azimuthal angle in the transverse plane. Including the renormalization factor \sqrt{S} from eq. (2) we get the renormalized effective coupling $g = \sqrt{S}g_0$ [12], which can be extracted from low energy data: we use $g^2/4\pi = 13.75$.

Because of the extended nature of the hadrons involved, the interaction in eq. (3) contains a phenomenological πNN form factor. It is important to stress here that while the vertex is derived from an effective meson-nucleon Lagrangian, the form factor is

introduced *ad hoc*. In order to parametrize the form factor we need to introduce the momentum transfer t which can be expressed as follows

$$t = (p_N - p'_N)^2 = -\frac{1}{z} [p_t^2 + (1-z)^2 m_N^2] = (1-z)(m_N^2 - M_{N\pi}^2) + m_\pi^2.$$

Different models and parametrizations are available in the literature. In the following we compare the results obtained using the light-cone approach and the covariant approach, the last one with inclusion of reggeization. Besides these two form factors we consider a πNN form factor extracted from Skyrme type models [13, 14]. This form factor leaves low momentum transfers essentially unaffected while suppressing the high momentum region strongly. The three models are:

- light-cone πNN form factor³

$$\begin{aligned} G(z, p_t) &= \exp[R_{lc}^2(m_N^2 - M_{N\pi}^2)] \\ &= \exp[R_{lc}^2(t - m_\pi^2)/(1-z)] \end{aligned} \quad (4)$$

- covariant πNN form factor

$$G(z, p_t) = \exp[R_c^2(t - m_\pi^2)] \quad (5)$$

- Skyrme model πNN form factor

$$G(z, p_t) = \exp[R_S^2 t] g(t) \quad (6)$$

where $g(t)$ is a rational function of t given in the appendix.

The amplitudes $\phi^{\lambda\lambda}$ are changed according to $\phi^{\lambda\lambda'} \rightarrow \phi^{\lambda\lambda'} G(z, p_t)$. The flux in eq. (1), for proton fragmentation into a neutron can then be calculated as

$$F_{n\pi}(z, p_t) = \frac{2}{3}\pi \sum_{\lambda\lambda'} |\phi_{N\pi}^{\lambda\lambda'}(z, \mathbf{p}_t)|^2 |G(z, p_t)|^2 \quad (7)$$

where 2/3 is the isospin factor and the azimuthal angle in the transverse plane has been integrated out. The reggeization of the pion (relevant for $z \rightarrow 1$) is included in the covariant and Skyrme approaches by the further change

$$\phi^{\lambda\lambda'} \rightarrow \phi^{\lambda\lambda'} (1-z)^{-\alpha_\pi(t)}$$

where $\alpha_\pi(t) = \alpha_\pi(0) + \alpha'_\pi t$ is the pion Regge trajectory, with $\alpha_\pi(0) = 0$ and $\alpha'_\pi \simeq 1 \text{ GeV}^{-2}$. The light-cone form factor contains the decrease of the cross section for $z \rightarrow 1$ already in the exponential. Its form, however, is a crude approximation and therefore we do not expect the light-cone form factor to be adequate for extremely large z .

In the following section we consider pp collisions in order to fix the parameters R_{lc} and R_c appearing in the previous equations⁴.

³We remind that this form factor is boost, but not Lorentz, invariant.

⁴For the Skyrme form factor we use the value fitted in [13]: $R_s^2 = 0.031/m_\pi^2$.

3 Estimate of absorptive corrections in $pp \rightarrow nX$

We consider target fragmentation reactions as stripping reactions in the cm-system where the projectile proton strips a π^+ from the target proton leaving behind a neutron. The projectile proton smashes the pion into pieces, but the neutron remains intact as a spectator. Any additional interactions like Δ -production or ρ -exchange may spoil this simple picture and reduce the accuracy of the determination of the πpn vertex. This has been studied and the amount of such a background is estimated to be around 20% [7, 8]. We will neglect these processes in our calculation, but we model them rescaling the one-pion exchange cross section by 1.2. The invariant differential cross section for the one pion exchange mechanism is (using light-cone amplitudes)

$$E_n \frac{d^3\sigma}{d^3\mathbf{p}_n} = \frac{z}{\pi} \frac{d\sigma}{dz dp_t^2} = \frac{2g^2}{16\pi^2} \frac{1}{z(1-z)} \frac{m_N^2(1-z)^2 + p_t^2}{(M_{N\pi}^2 - m_N^2)^2} |G(z, p_t)|^2 \sigma_{\text{tot}}^{p\pi}. \quad (8)$$

This picture is reliable when the pion and the neutron in the *target* proton are well separated, i.e. at large z and large impact parameter. For small impact parameters and intermediate z values it must be extended to allow the scattering of the projectile on the neutron and the consequent screening effect (see fig. 2).

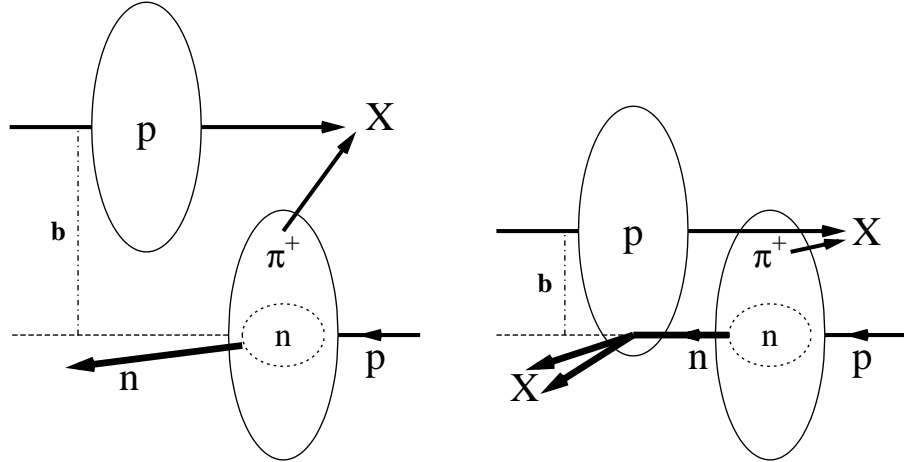


Figure 2: *Picture of the collision for two different impact parameters. On the left we show a peripheral collision (large \mathbf{b}) where the pion is stripped and the neutron acts as a spectator. On the right we show a more central collision where the projectile proton can destroy the neutron through rescattering.*

To be more precise we distinguish in our notation between the target ($p_{(T)}$) and projectile ($p_{(P)}$) proton:

$$p_{(P)} p_{(T)} \rightarrow nX.$$

We employ the high energy Glauber approximation to multiple scattering which has been used for target fragmentation in heavy ion collisions in ref. [15]. We treat the target proton as a pion-neutron system (ϕ_0) undergoing a transition to an excited state (ϕ_α).

The cross section for this process can be expressed as

$$\sigma(\phi_0 \rightarrow \phi_\alpha) = \int d^2\mathbf{b} |\langle \phi_\alpha [1 - S^{p\pi} S^{pn}] | \phi_0 \rangle|^2 = \int d^2\mathbf{b} \sigma_{0 \rightarrow \alpha}(\mathbf{b}), \quad (9)$$

where \mathbf{b} is the impact parameter, and S^{ab} are the interaction operators (see below). We assume that the proton state ϕ_0 can be factorized into a system of a pion and a neutron

$$|\phi_0\rangle \equiv |\psi_0^{sp}\pi_0n_0\rangle = |\psi_0^{sp}\rangle|\pi_0\rangle|n_0\rangle,$$

with ψ_0^{sp} the spatial component (to keep spatial and intrinsic degrees of freedom separated). Similarly the excited state with an undisturbed neutron has the form:

$$|\phi_\alpha\rangle \equiv |\psi_j^{sp}\pi_{\alpha'}n_0\rangle = |\psi_j^{sp}\rangle|\pi_{\alpha'}\rangle|n_0\rangle$$

where we have introduced an extra index (j) to take into account all possible spatial configurations for this excited state; $|\pi_{\alpha'}\rangle$ is an arbitrary state with the same quantum numbers as the pion. To get the total cross section we sum now over all spatial configurations and over all $|\pi_{\alpha'}\rangle$ states. We apply the closure relations and exclude the elastic contribution ($|\pi_0\rangle$)

$$\begin{aligned} \sigma(\mathbf{b}) &= \sum_\alpha \sigma_{0 \rightarrow \alpha}(\mathbf{b}) \\ &= \sum_{\alpha' \neq 0} \sum_j \left| \int d^3x_n d^3x_\pi \psi_j^*(x_n, x_\pi) \psi_0(x_n, x_\pi) S_{\alpha'0}^{p\pi}(\mathbf{b} - \mathbf{s}_\pi) S_{00}^{pn}(\mathbf{b} - \mathbf{s}_n) \right|^2 \\ &= \sum_{\alpha' \neq 0} \int d^3x_n d^3x_\pi |\psi_0(x_n, x_\pi)|^2 S_{\alpha'0}^{p\pi}(\mathbf{b} - \mathbf{s}_\pi) S_{0\alpha'}^{\dagger p\pi}(\mathbf{b} - \mathbf{s}_\pi) |S_{00}^{pn}(\mathbf{b} - \mathbf{s}_n)|^2 \quad (10) \\ &= \int d^3x_n d^3x_\pi |\psi_0(x_n, x_\pi)|^2 \left[1 - |S_{00}^{p\pi}(\mathbf{b} - \mathbf{s}_\pi)|^2 \right] |S_{00}^{pn}(\mathbf{b} - \mathbf{s}_n)|^2 \end{aligned}$$

where $x_n \equiv (\mathbf{s}_n, z_n)$, $x_\pi \equiv (\mathbf{s}_\pi, z_\pi)$, \mathbf{s}_π and \mathbf{s}_n are the coordinates of the pion and the neutron in the impact parameter plane; z_n and z_π are their longitudinal momentum fractions. Also

$$1 - |S_{00}^{p\pi}|^2 = 1 - |1 - \Gamma^{p\pi}|^2 \simeq 2\text{Re}\Gamma^{p\pi} \quad |S_{00}^{pn}|^2 = |1 - \Gamma^{pn}|^2 \simeq 1 - 2\text{Re}\Gamma^{pn} \quad (11)$$

where the profile functions Γ describe the respective two body scatterings and are related to the scattering amplitude in momentum space by Fourier transformation

$$f^{ij}(\mathbf{q}) = \frac{ip_{\text{cm}}}{2\pi} \int d^2\mathbf{b} e^{i\mathbf{q} \cdot \mathbf{b}} \Gamma^{ij}(\mathbf{b}). \quad (12)$$

Let us now consider the density distribution $|\psi_0(x_n, x_\pi)|^2$. We parametrize this density starting from the probability density to find a pion and a neutron at a certain transverse separation $\mathbf{b}_{\text{rel}} = \mathbf{s}_n - \mathbf{s}_\pi$, imposing the center-of-mass constraint in \mathbf{b} -space and the longitudinal momentum conservation

$$\mathbf{b}_{\text{cm}} = z_n \mathbf{s}_n + z_\pi \mathbf{s}_\pi = 0 \quad z_n + z_\pi = 1,$$

i.e.

$$|\psi_0(x_n, x_\pi)|^2 \equiv \rho_{n\pi}(z_n, \mathbf{b}_{rel}) \delta^2(z_n \mathbf{s}_n + z_\pi \mathbf{s}_\pi) \delta(z_n + z_\pi - 1). \quad (13)$$

Inserting eqs. (11) and (13) into eq. (10) and carrying out the 3-dimensional x_π integration, we get for the semi-inclusive cross section

$$\frac{d\sigma^{pp \rightarrow nX}}{dz} = \int d^2\mathbf{b} \frac{d\sigma(\mathbf{b})}{dz} \quad \text{with} \quad (14)$$

$$\begin{aligned} \frac{d\sigma(\mathbf{b})}{dz} &= \int d^2\mathbf{s}_n \frac{1}{(1-z)^2} \rho_{n\pi}(z, \mathbf{b}_{rel}) 2\text{Re}\Gamma^{p\pi}(\mathbf{b} - \mathbf{s}_\pi) [1 - 2\text{Re}\Gamma^{pn}(\mathbf{b} - \mathbf{s}_n)] \\ &= \int d^2\mathbf{b}_{rel} \rho_{n\pi}(z, \mathbf{b}_{rel}) 2\text{Re}\Gamma^{p\pi}(\mathbf{b} + z\mathbf{b}_{rel}) [1 - 2\text{Re}\Gamma^{pn}(\mathbf{b} - (1-z)\mathbf{b}_{rel})], \end{aligned} \quad (15)$$

where we have restored the previous notation, $z_n \equiv z$ and replaced the pion and neutron coordinates by

$$\mathbf{b}_{rel} = -\frac{\mathbf{s}_\pi}{z} = \frac{\mathbf{s}_n}{1-z}.$$

3.1 Pion-neutron density and profile functions in \mathbf{b} space

In order to extract quantitative information from eq. (15) we evaluate the probability density to find a pion and neutron at a certain distance inside the parent proton. The main idea is to start with the amplitudes in momentum space for the splitting of a proton into a pion-neutron system (see eqs. (3)) and then calculate the Fourier transform in two dimensions with respect to the transverse momentum. We obtain the amplitudes in \mathbf{b} -space (we keep z fixed)

$$\psi_{n\pi}^i(z, \mathbf{b}_{rel}) = \frac{1}{2\pi} \int d^2\mathbf{p}_t e^{i\mathbf{b}_{rel} \cdot \mathbf{p}_t} \phi_{n\pi}^i(z, \mathbf{p}_t),$$

where by $\phi_{n\pi}^i$ we mean $\sqrt{2/3}\phi_{N\pi}^{\lambda\lambda'}$. From this we obtain the probability density to find a neutron and a pion respectively with longitudinal momentum z and $1-z$ and relative transverse separation \mathbf{b}_{rel} :

$$\rho_{n\pi}(z, \mathbf{b}_{rel}) = \sum_i |\psi_{n\pi}^i(z, \mathbf{b}_{rel})|^2.$$

In fig. 3 we show the behaviour of these densities at different values of z for the light-cone and the covariant approach.

Concerning the profile functions we start from scattering amplitudes with gaussian shapes,

$$f^{ab}(\mathbf{q}) = \frac{ip_{cm}}{4\pi} \sigma_{tot}^{ab} \exp\left[-\frac{\mathbf{q}^2}{2\Lambda_{ab}^2}\right] \quad (16)$$

and by Fourier transformation we get

$$\Gamma^{ab}(\mathbf{b}) = \frac{1}{4\pi} \sigma_{tot}^{ab} \Lambda_{ab}^2 \exp\left[-\frac{\mathbf{b}^2 \Lambda_{ab}^2}{2}\right] \quad (17)$$

where we have considered purely imaginary amplitudes as we are interested in the high-energy regime.

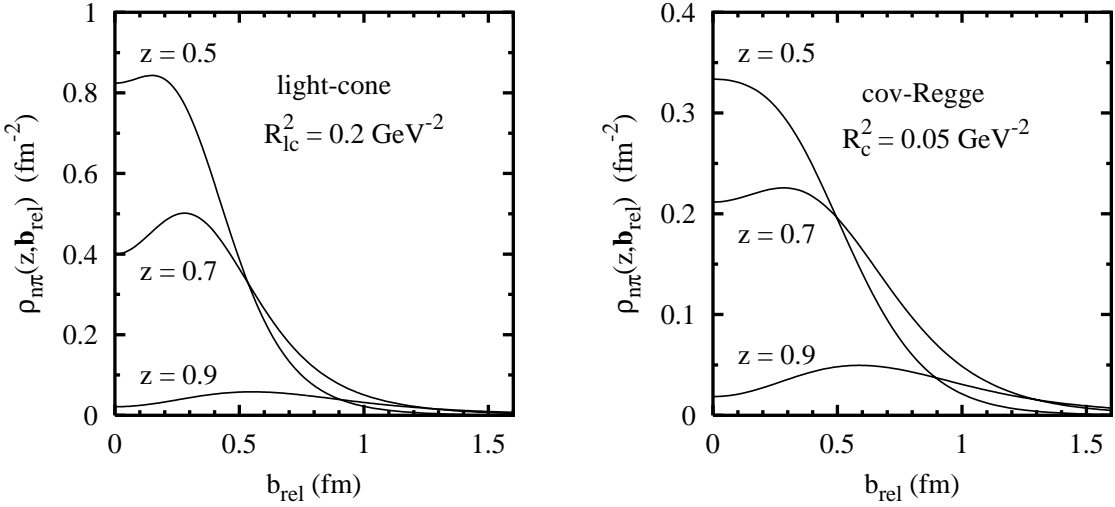


Figure 3: Pion-neutron densities in the transverse plane for various z values in light-cone approach (left) and covariant approach (right).

3.2 Cross section for $pp \rightarrow nX$

The gaussian dependence of the profile functions allows us to perform the \mathbf{b} integration in eq. (14) analytically, we have then

$$\frac{d\sigma^{pp \rightarrow nX}}{dz} = \int d^2\mathbf{b}_{rel} \rho_{n\pi}(z, \mathbf{b}_{rel}) \sigma_{tot}^{p\pi} \left\{ 1 - \Lambda_{eff}^2 \frac{\sigma_{tot}^{pn}}{2\pi} \exp \left[-\frac{\Lambda_{eff}^2 \mathbf{b}_{rel}^2}{2} \right] \right\} \quad (18)$$

with

$$\Lambda_{eff}^2 = \frac{\Lambda_{p\pi}^2 \Lambda_{pn}^2}{\Lambda_{p\pi}^2 + \Lambda_{pn}^2} \quad [\Lambda_{p\pi}^2 \approx \Lambda_{pn}^2 \approx 0.08 \text{ GeV}^2] \quad (19)$$

Before giving explicit results applying eq. (18), let us try to interpret the physical picture emerging from it.

The first term alone is nothing else than the standard expression according to the factorization hypothesis, eq. (1), i.e. the stripping of the pion cloud inside the target proton. The second term represents the screening correction which is the most interesting result of our calculation. The Born fragmentation cross section is multiplied by the probability that the projectile proton does not destroy the neutron component of the target proton. The screening factor changes the simple factorization picture.

Assuming that the final state interaction does not modify the transverse momentum distribution of the fragments, we can calculate the invariant differential cross section $E_n \frac{d^3\sigma}{d^3\mathbf{p}_n}$ by multiplying the differential cross sections for the longitudinal distributions with the transverse probability distribution for the fragmentation process (see eq. (8)). This method seems to work quite well in nuclear target fragmentation [15]. We get

$$E_n \frac{d^3\sigma^{pp \rightarrow nX}}{d^3\mathbf{p}_n} = \frac{z}{\pi} \frac{1}{N(z)} \frac{dN(z, p_t)}{dp_t^2} \frac{d\sigma^{pp \rightarrow nX}}{dz} \quad (20)$$

where $d\sigma/dz$ is given by eq. (18). The normalized fraction of fragmentation processes in the interval $p_t, p_t + dp_t$ is obtained from the normalized pion flux factor:

$$\frac{1}{N(z)} \frac{dN(z, p_t)}{dp_t^2} = \frac{F_{n\pi}(z, p_t)}{\int dp_t^2 F_{n\pi}(z, p_t)}. \quad (21)$$

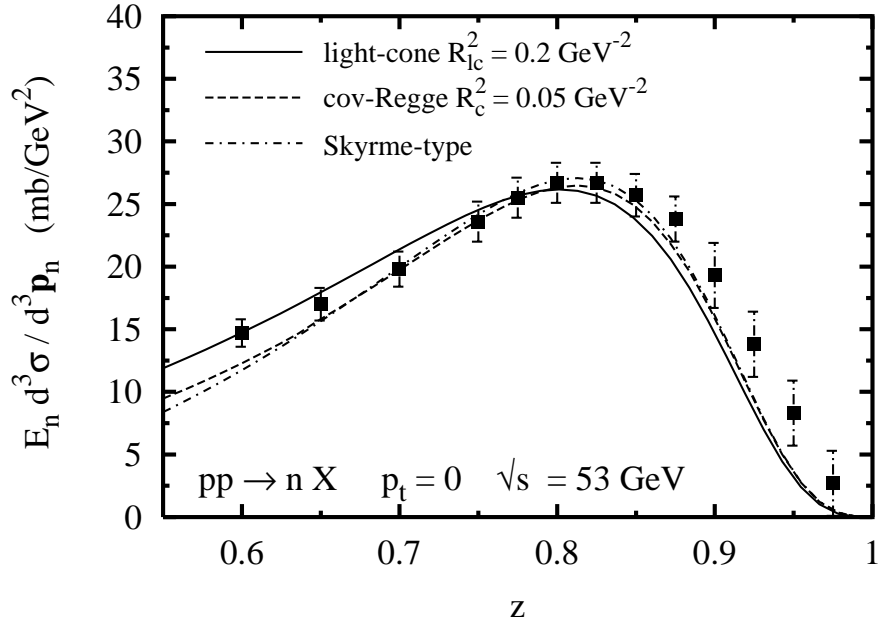


Figure 4: *Invariant differential cross sections for neutron production at $p_t = 0$ calculated according to eq. (20) for three different form factors. Data points are from ref. [16].*

Definitely the experimental cross sections for $p_t = 0$ [16, 17] have the most pronounced shape. Here one can really see a fragmentation peak which seems to be superimposed on some background. We estimate the background to have the same shape as the cross section we calculated and to lead to a 20% correction. Thus we scale all results for the cross section by a factor 1.2. The additional contributions thus parametrized may come from resonance excitations like $p \rightarrow \pi^+ \Delta^0$ and $p \rightarrow \pi^+ N^{*0}$, which decay into neutrons. For larger p_t values the fragmentation cross sections become rapidly flatter and smaller, probably also the background increases. Therefore we fit the radius parameters to the $p_t = 0$ data. In fig. 4 we show the semi-inclusive cross section for $pp \rightarrow nX$ as a function of the longitudinal momentum fraction z of the neutron together with the experimental data from ref. [16]. For the total cross sections $\sigma^{p\pi}$ and σ^{pn} we adopt the fits performed in ref. [18]. We adjust the radius parameters R_{lc} in the light-cone and R_c in the covariant form factor to the data. We find a reasonable agreement with the data for a radius squared $R_{lc}^2 = 0.2 \text{ GeV}^{-2}$ in the light-cone form factor and $R_c^2 = 0.05 \text{ GeV}^{-2}$ for the covariant Regge parametrization respectively. An important feature of the screening correction is that it reduces the radius parameters. The shape of the Skyrme form factor does not deviate appreciably from the covariant form factor, because even at smaller values of z

the momentum transfers $|t|$ in fig. 4 are not large. One should also keep in mind that the reggeized pion has a variable spin different from zero, when t is different from the pole value. The coupling of virtual pions to the nucleon does not have to be identical to that employed in one pion exchange potentials.

The differences of the light-cone and covariant approaches are more pronounced for very large z and at $p_t \neq 0$, cf. fig. 5. Here the light-cone form factor vanishes faster with z compared to the fall off in the reggeized covariant form factor. In fig. 5 we compare the light-cone, the covariant-Regge and the Skyrme-type models with the invariant differential cross sections measured at $p_t = 0.2$ GeV [17]. The theory does not agree very well with these data. In fact these data are taken at $\sqrt{s} = 6.84$ GeV, where Feynman scaling is not expected to hold. There are also data at larger energies [21], but these do not cover simultaneously the large z and small p_t range.

The effect of screening is shown clearly in fig. 6, where we plot the K -factor, i.e. the ratio of the differential cross section with and without absorptive correction for the fitted values of the radii. The individual models differ slightly in the $z < 0.7$ region where there is a sizeable, $> 30\%$, screening. The light-cone form factor leads to a slightly smaller K -factor. For very large z values large transverse separations between the neutron and the pion dominate (see fig. 3), thus the projectile proton misses the neutron for almost any finite impact parameter and the K -factor approaches unity.

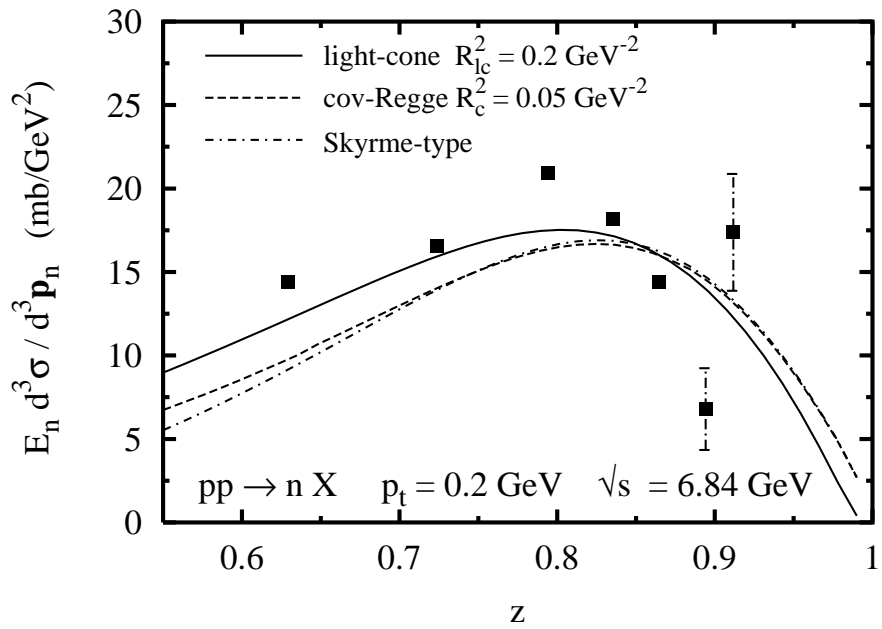


Figure 5: *Invariant differential cross sections for neutron production at $p_t = 0.2$ GeV calculated according to eq. (20) for three different form factors. Points are low energy $\sqrt{s} = 6.84$ GeV bubble chamber data, ref. [17].*

A comparison of the data with a calculation neglecting the screening mechanism, would give larger radii. Such a fit can represent the data down to lower z values like

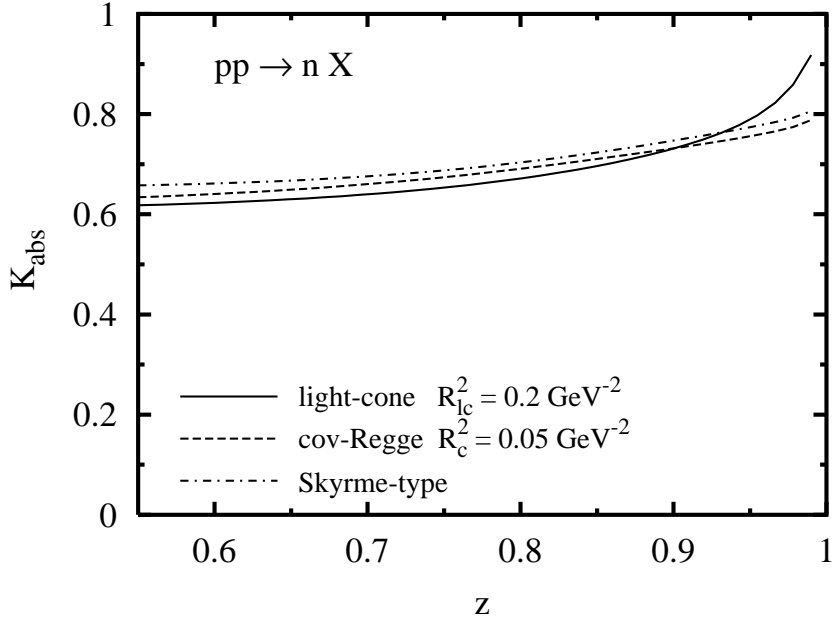


Figure 6: *Absorptive K-factors for neutron production in proton-proton collisions for three different form factors.*

$z = 0.65$. We think, however, that other reaction mechanisms are important in a region where two valence quarks can fragment into a final neutron.

4 Cross sections for $\gamma^* p \rightarrow nX$ and $\gamma p \rightarrow nX$

In this section we consider the interaction of an initial real or virtual photon with the proton leading to neutron target fragments. Before entering the detailed calculation of the semi-inclusive reaction it is worth-while to make some remarks on inclusive photon nucleon interaction in context with our πNN form factor. Recently [14] an estimate of the antiquark distributions in the nucleon has been performed with the help of the Sullivan formula cf. eq. (1). The calculation shows that for the Skyrme form factor used above the MCM prediction exhausts or only slightly exceeds the light sea quark distributions \bar{u} and \bar{d} in the proton at $Q^2 = 1.2 \text{ GeV}^2$. This is a large improvement with respect to harder form factors often used before, which strongly overestimate this contribution. Thus the problems discussed e.g. in ref. [12] seem to be well taken care of. Two comments are in place: perhaps the F_2 calculations are not valid because of the interference between photon nucleon and photon pion inelastic interactions, where the target like slow fragments of the struck sub-hadron and the residual hadron interact. Since both are slow and strongly interacting there is no reason that this final state interaction is negligible. A second remark about the pion pole calculation is the possible contribution of diffractive excitation of the proton feeding the neutron channel. This problem has to be sorted out by a calculation of the Pomeron exchange contribution.

Preliminary experiments [10] rather point to the fact that for $z < 0.8$ there is a sizable contribution of π_0 exchange to forward proton production.

In the semi-inclusive reaction we limit ourselves mainly to forward neutrons in photon induced reactions at small x_{Bj} , as they are studied at HERA. In this kinematic region one cannot apply the usual factorization into a photon quark cross section times a distribution function multiplied by a quark fragmentation function. That is why it is interesting by itself to study target fragmentation as a nonperturbative process combining fragmentation and structure information. With good reason the new concept of fracture functions has been invented for this process. For small x_{Bj} we can consider the photon as a quark antiquark state which materialises long before it reaches the proton and interacts with the pion and neutron in the proton wave function. Schematically we write the inelastic cross section in a form similar to the proton induced one:

$$\sigma(\phi_0 \rightarrow \phi_\alpha) = \int d^2\mathbf{b} dw d^2\mathbf{r} |\Psi_{q\bar{q}}(w, \mathbf{r})|^2 |\langle \phi_\alpha [1 - S^{q\bar{q}\pi} S^{q\bar{q}n}] | \phi_0 \rangle|^2 \quad (22)$$

Here the $q\bar{q}$ pair wave function is represented by $|\Psi_{q\bar{q}}(w, \mathbf{r})|^2$ with w being the momentum fraction of the quark and \mathbf{r} the transverse separation of the quarks. This wave function contains the summation over the electric charges of the different quarks and is electromagnetic in origin. The weak electromagnetic coupling determines the cross section of the photon with the pion.

Following the same procedure for the sum over all spatial configurations and over all excited (inelastic) states we get

$$\frac{d\sigma^{\gamma^* p \rightarrow nX}}{dz} = \int d^2\mathbf{b}_{rel} \rho_{n\pi}(z, \mathbf{b}_{rel}) \int d^2\mathbf{b} dw d^2\mathbf{r} \left\{ |\Psi_{q\bar{q}}(w, \mathbf{r})|^2 2\text{Re}\Gamma^{q\bar{q}\pi}(\mathbf{b} - \mathbf{s}_\pi - \mathbf{r}) [1 - 2\text{Re}\Gamma^{q\bar{q}n}(\mathbf{b} - \mathbf{s}_n - \mathbf{r})] \right\}. \quad (23)$$

In this form we can see the role played by the photon wave function: it governs the integral but does not influence the magnitude of the screening correction, which is entirely given by the $q\bar{q}$ cross section with the neutron. Screening is therefore a strong interaction effect which is a function of the transverse size of the $q\bar{q}$ pair. Mathematically we use the mean value theorem and evaluate the screening at the maximum value of the photon pion cross section. Otherwise we calculate the differential cross section in the same manner as before and get

$$\frac{d\sigma^{\gamma^* p \rightarrow nX}}{dz} = \int d^2\mathbf{b}_{rel} \rho_{n\pi}(z, \mathbf{b}_{rel}) \sigma_{tot}^{\gamma^* \pi} \left\{ 1 - \Lambda_{eff}^2 \frac{\sigma_{tot}^{q\bar{q}n}}{2\pi} \exp \left[-\frac{\Lambda_{eff}^2 \mathbf{b}_{rel}^2}{2} \right] \right\} \quad (24)$$

with

$$\Lambda_{eff}^2 = \frac{\Lambda_{q\bar{q}\pi}^2 \Lambda_{q\bar{q}n}^2}{\Lambda_{q\bar{q}\pi}^2 + \Lambda_{q\bar{q}n}^2} \quad (25)$$

where for the profile functions we have again restricted ourselves to gaussian shapes. For the double differential cross section, see eqs. (20) and (21),

$$\frac{d^2\sigma^{\gamma^* p \rightarrow nX}}{dz dp_t^2} = \frac{1}{N(z)} \frac{dN(z, p_t)}{dp_t^2} \frac{d\sigma^{\gamma^* p \rightarrow nX}}{dz}, \quad (26)$$

and eventually the differential cross section for neutron production in electron-proton scattering is obtained through

$$\frac{d^4\sigma^{ep \rightarrow e'nX}}{dx_{Bj}dQ^2dzdp_t^2} = \frac{\alpha_{em}}{2\pi x_{Bj}Q^2} (2 - 2y + 2y^2) \frac{d^2\sigma^{\gamma^*p \rightarrow nX}}{dzdp_t^2}, \quad (27)$$

with $x_{Bj} = \frac{Q^2}{2q \cdot p}$, $y = \frac{Q^2}{x_{Bj}s}$; s is the cm ep total energy squared.

The total cross sections $\sigma_{tot}^{\gamma^*\pi}$ and $\sigma_{tot}^{q\bar{q}n}$ appearing in eq. (24) are functions of Q^2 and of the scaling variables, respectively, $x_\pi = x_{Bj}/(1 - z)$ and $x_n = x_{Bj}/z$,

$$\sigma_{tot}^{\gamma^*\pi} = \sigma_{tot}^{\gamma^*\pi}(x_\pi, Q^2) \quad \sigma_{tot}^{q\bar{q}n} = \sigma_{tot}^{q\bar{q}n}(x_n, Q^2). \quad (28)$$

Besides, we have

$$\sigma_{tot}^{\gamma^*\pi}(x_\pi, Q^2) = \frac{4\pi^2\alpha_{em}}{Q^2} F_2^\pi(x_\pi, Q^2). \quad (29)$$

The above equation gives the virtual photon-pion cross section in terms of the pion structure function. In the following we use $F_2^\pi(x_{Bj}, Q^2) = \frac{2}{3}F_2^p(x_{Bj}, Q^2)$ at $x_{Bj} \ll 0.1$.

Another ingredient in eq. (24) is the $q\bar{q}n$ cross section, which we parametrize as

$$\sigma_{tot}^{q\bar{q}n}(x_n, Q^2) = \sigma_{tot}^{\rho n} \frac{\sigma^{\gamma^*n}(x_n, Q^2)}{\sigma^{\gamma n}(Q^2 = 0)}. \quad (30)$$

Phenomenologically we estimate this strong interaction cross section by scaling the ρn cross section with the decreasing size of the quark-antiquark pair as it manifests itself in the photon cross section. This approach is justified with the caveat that in the transverse photon there is also some amount of large size dipoles with quark momentum fraction w close to zero. Since we do not separately integrate over the w variable in the dipole wave function we use this phenomenological approximation. Working at small x_{Bj} we can exchange all neutron labels in the above formula against proton labels. The unknown ρ cross section is taken as the πn cross section. For the γ^*n cross section we use the parametrization in the double leading log approximation [19] which covers a wide x_{Bj} and Q^2 range. For the photoproduction cross section we use the interpolation formula by Donnachie and Landshoff [18] connecting the small $\sqrt{s} = 10$ GeV region with the data points near $\sqrt{s} = 200$ GeV.

For the slope parameters $\Lambda_{q\bar{q}\pi}^2$ and $\Lambda_{q\bar{q}n}^2$ we use a geometrical picture that allows us to relate these to the total cross sections for the $q\bar{q}$ pair scattering on pion and neutron targets. In this way we include the effect of the photon virtuality, not only in the magnitude but also into the range of the $q\bar{q} - \pi$ and $q\bar{q} - n$ interactions:

$$\Lambda_{q\bar{q}\pi}^2 \approx \frac{4\pi}{\sigma_{tot}^{q\bar{q}\pi}} \quad \Lambda_{q\bar{q}n}^2 \approx \frac{4\pi}{\sigma_{tot}^{q\bar{q}n}}.$$

The so parametrized cross section of the colour dipole in the photon with the neutron becomes smaller with increasing virtuality of the photon. Practically there is no screening for $Q^2 > 5$ GeV 2 . To show this we plot in fig. 7 the integrated neutron energy distributions in photoproduction with $5 \text{ GeV} < E_e < 22 \text{ GeV}$, $Q^2 < 0.02 \text{ GeV}^2$, and in deep inelastic

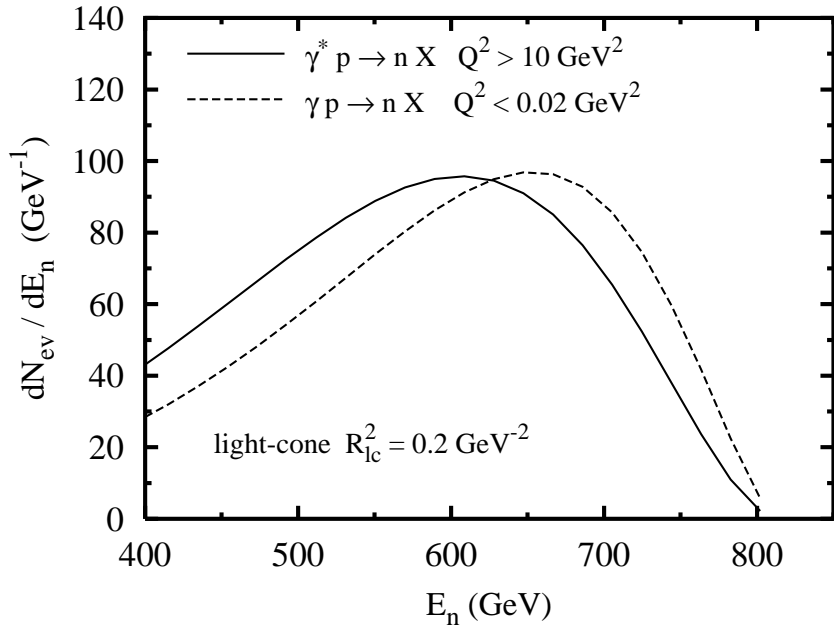


Figure 7: *Comparison of the energy distributions of neutrons for deep inelastic events and photoproduction imposing the kinematical cuts of ref. [1]. The distributions are normalized to the total number of DIS events.*

scattering with $0.04 < y < 0.95$, $Q^2 > 10 \text{ GeV}^2$, the ZEUS cuts ($\theta_{\text{scat}} < 0.6 \text{ mrad}$, $p_t < 0.5 \text{ GeV}$ and an integrated luminosity of 6.7 pb^{-1}). A shift of the DIS cross section maximum by 50 GeV to lower energies is clearly visible. This is due to screening, which reduces the cross section at smaller z , such that the peak appears at higher energies in photoproduction. Remarkably our results show a clear signal for color transparency in the proton. Small size color dipoles do not rescatter on the target fragment neutron. The inclusive reaction opens the possibility to study this QCD effect of the nucleon without some of the complications of nuclei. The absorptive K -factors for $\gamma p \rightarrow n X$ and $ep \rightarrow e'nX$ is shown in fig. 8: it is visible that for DIS neutron production (high Q^2) screening becomes negligible, while for real photons we get more or less the same effect as in proton-proton collisions (see fig. 6). For $z > 0.75$ and $Q^2 > 10 \text{ GeV}^2$ the factorization of the cross section into a pion flux factor and a pion structure functions looks very acceptable.

In fig. 9 we show the p_t -integrated neutron cross section with the $H1$ cuts as function of z . The screening in $pp \rightarrow nX$ manifests itself as a bigger $ep \rightarrow e'nX$ cross section, since a higher pion flux is needed to explain the measured hadronic cross section. Notwithstanding the validity of the impuls approximation in high Q^2 processes, factorization is broken in soft hadronic fragmentation reactions. The comparison of our result with the preliminary $H1$ data is very encouraging.

The fracture functions [3, 4] introduced to describe target fragmentation allow a model independent evolution in the framework of perturbative QCD, albeit the starting

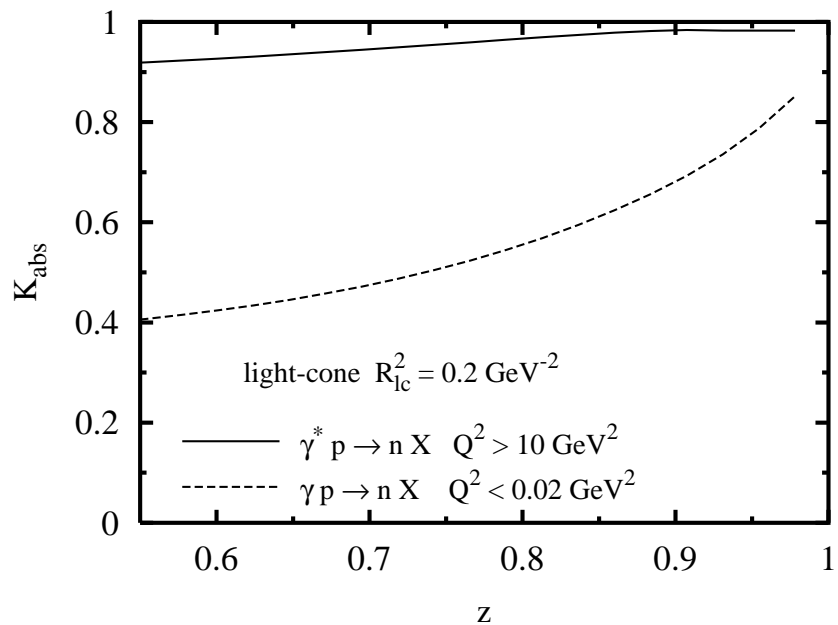


Figure 8: *Absorptive K-factor for neutron production in real and virtual photon-proton collisions.*

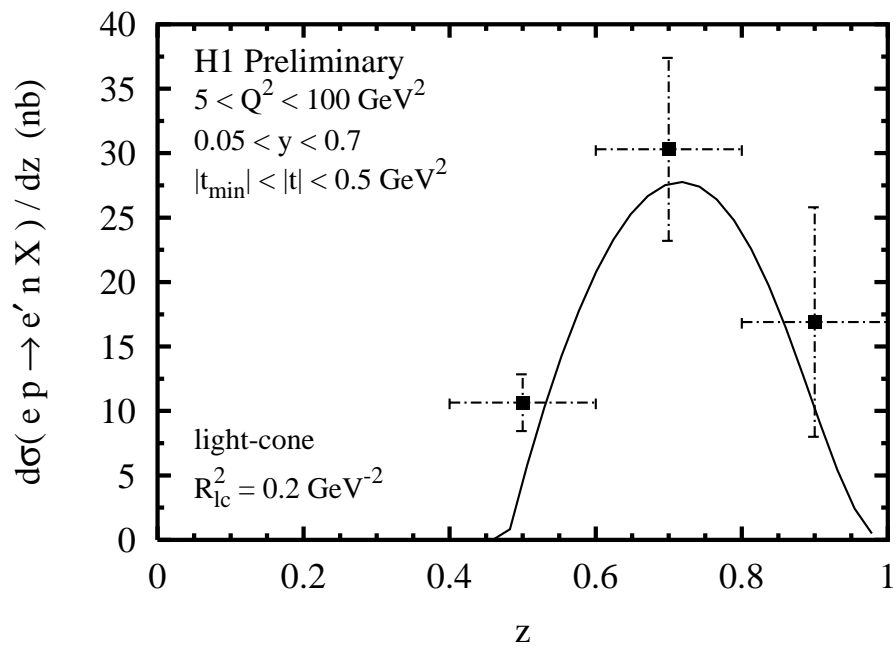


Figure 9: *Comparison of the differential cross section including screening corrections in light-cone approach with preliminary H1 data, ref. [2].*

functions have to be known. In this approach the non-perturbative distributions are related to the p_t -integrated differential cross section for leading neutron production in ep scattering in the following way

$$\frac{d^3\sigma^{ep \rightarrow e'nX}}{dx_{Bj}dQ^2dz} = \frac{2\pi\alpha_{em}^2}{x_{Bj}Q^4}(2-2y+2y^2) M_2(x_{Bj}, Q^2, z) \quad (31)$$

where at leading order in α_s there is no contribution from the fragmentation of the struck quark in the target region. In the one pion exchange model without screening corrections one can interpret⁵ $M_2(x_{Bj}, Q^2, z)$ as the product of the flux of neutrons integrated over p_t , times the pion structure function $F_2^\pi(x_\pi, Q^2)$.

The distribution $M_2(x_{Bj}, Q^2, z)$ is defined in analogy with the structure function $F_2(x_{Bj}, Q^2)$,

$$M_2(x_{Bj}, Q^2, z) = x_{Bj} \sum_i e_i^2 M_{i,n/p}(x_{Bj}, Q^2, z) \quad (32)$$

where $M_{i,n/p}(x_{Bj}, Q^2, z)$ represents the probability of finding a parton of flavour i with momentum fraction x_{Bj} and a neutron with momentum fraction z inside a proton.

In fig. 10 we give the fracture functions $M_2(x_{Bj}, Q^2, z)$ as functions of z , at fixed x_{Bj} , for various Q^2 values.

The Q^2 evolution of the fracture functions we use is given at small virtualities by the higher twist effect of screening and at higher Q^2 by the evolution of the pion structure function. In fact for neutron fragmentation the Altarelli-Parisi evolution of the fracture function dominates the total Q^2 dependence as has been argued in ref. [20].

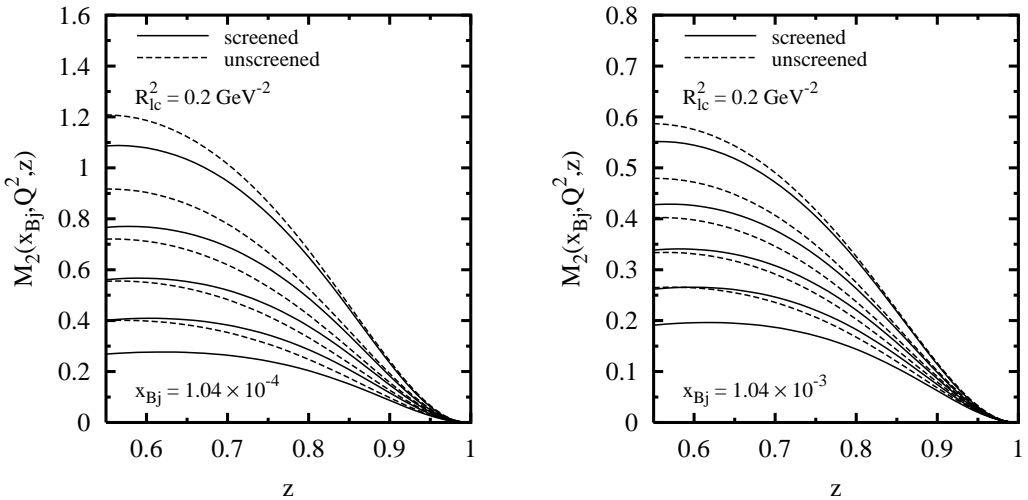


Figure 10: Q^2 -evolution of fracture functions $M_2(x_{Bj}, Q^2, z)$ at fixed x_{Bj} as function of z . The Q^2 values are (from bottom to top) 2.5, 4.4, 7.5, 13.3, 28.6 GeV^2 .

⁵Here one should consider this fracture function as an input distribution at a certain scale Q_0^2 and then apply the pQCD-evolution.

5 Discussion of fragmentation results and validity of the factorization hypothesis

Finally we compare the screening corrections for the three different cases of proton, real and DIS photon induced semi-inclusive fragmentation reactions (cf. figs. 6, 8). One sees that both proton induced and real photon induced cross sections have K -factors differing by about thirty percent from unity for $z < 0.8$. In this region factorization for these reactions does not hold. This makes a model independent extraction of the photon-pion cross section difficult for these z values. On the other hand for deep inelastic scattering at $Q^2 > 10 \text{ GeV}^2$ the rescattering of the $q\bar{q}$ dipole in the photon by the neutron is unimportant. Nevertheless an extraction of the pion structure function is affected by the uncertainty in the determination of the pion flux factor. Our fits to the proton induced fragmentation reaction give for the radius parameters $R_{lc}^2 = 0.2 \text{ GeV}^{-2}$ and $R_c = 0.05 \text{ GeV}^{-2}$. More accurate p_t neutron spectra in the case of deep inelastic scattering could reduce this uncertainty significantly. At the moment the p_t spectra in proton induced reactions have been measured for too low energies [17] or too high p_t in the relevant z range [21].

It may be added that other mechanisms in all three reactions start contributing for $z < 0.75$. Previously ρ exchange [7, 8] has been added to the strong proton induced cross section presenting a non negligible contribution for $0.5 < z < 0.7$. In Monte Carlo simulations (lepto) the fragmentation cross section increases for $z < 0.5$. Further work is needed to understand this part of the cross section theoretically.

The semi-inclusive reactions in the large z -region show yet another case of color transparency. We think this finding of our paper merits a more accurate experimental examination. Exclusive (e.g. ρ production) reactions are in good agreement with theoretical calculations based on the dipole picture, which is underlying color transparency. But without nuclear targets there is no clear proof of this phenomenon. With semi-inclusive neutron fragmentation, however, even for a single nucleon a new channel is available to study final state interactions of virtual partons.

Acknowledgments

We thank J. Hüfner, B. Kopeliovich, B. Povh, D. Jansen and T. Nunnemann for valuable discussions. A.S. acknowledges support by BMBF.

Appendix

Here we give the expression for the function entering in the Skyrme-type form factor, eq. (6), [22]:

$$g(x) = 1 + \frac{\sum_{k=0}^3 a_k T_k(\bar{x})}{1 + mx}, \quad x = \frac{|t|}{m_\pi^2}, \quad \bar{x} = \frac{2x - a - b}{b - a} \quad (33)$$

where T_k is the k -th Tchebycheff polynomial of 1st kind, with
 $a = 0.003113 \quad b = 280.198488 \quad m = 10^{-8}$,

$$a_0 = 6.242336 \quad a_1 = 4.940353 \quad a_2 = 2.740654 \quad a_3 = 0.9217577 .$$

References

- [1] Zeus collab., M. Derrick et al., Phys. Lett. **B 384** (1996) 388.
- [2] H1 collab., Europhysics Conf. on High Energy Physics (378) Jerusalem 1997.
- [3] L. Trentadue and G. Veneziano, Phys. Lett. **B 323** (1994) 201.
- [4] D. Graudenz, Nucl. Phys. **B 432** (1994) 351.
- [5] J.D. Sullivan, Phys. Rev. **D 5** (1972) 1732.
- [6] M. Bishari, Phys. Lett. **B 38** (1972) 510.
- [7] H. Holtmann, G. Levman, N.N. Nikolaev, A. Szczurek and J. Speth, Phys. Lett. **B 338** (1994) 363.
- [8] B.Z. Kopeliovich, B. Povh and I. Potashnikova, Z. Phys. **C 73** (1996) 125.
- [9] N.N. Nikolaev, J. Speth and B. G. Zakharov, hep-ph/9708290.
- [10] D. Jansen and T. Nunnemann, private communication.
- [11] H. Holtmann, A. Szczurek and J. Speth Nucl Phys. **A 596** (1996) 631.
- [12] W. Koepf, L. L. Frankfurt and M. Strikman, Phys. Rev. **D 53** (1996) 2586.
- [13] G. Holzwarth and R. Machleidt, Phys. Rev. **C 55** (1997) 1088.
- [14] R. J. Fries and A. Schäfer, preprint hep-ph/9801358.
- [15] A.Y. Abul-Magd and J. Hüfner, Nucl. Phys. **A 308** (1978) 429.
- [16] W. Flauger and F. Mönnig, Nucl. Phys. **B 109** (1976) 347.
- [17] V. Blobel et al., Nucl. Phys. **B 135** (1978) 379.
- [18] A. Donnachie and P.V. Landshoff, Phys. Lett. **B 296** (1992) 227.
- [19] B.Z. Kopeliovich and B. Povh, Phys. Lett. **B 367** (1996) 329.
- [20] D. de Florian and R. Sassot, preprint hep-ph/9703228.
- [21] J. Engler et al., Nucl. Phys. **B 84** (1975) 70.
- [22] R. J. Fries, private communication.